Nariai, Bertotti-Robinson, and anti-Nariai solutions in higher dimensions

Vitor Cardoso*
Centro Multidisciplinar de Astrofísica, CENTRA, Departamento de Física, Instituto Superior Técnico, Av. Rovisco Pais 1, 1049-001 Lisbon, Portugal and Centro de Física Computacional, Universidade de Coimbra, P-3004-516 Coimbra, Portugal

Óscar J. C. Dias†
Centro Multidisciplinar de Astrofísica, CENTRA, Departamento de Física, Instituto Superior Técnico, Av. Rovisco Pais 1, 1049-001 Lisbon, Portugal and CENTRA, Departamento de Física, F.C.T., Universidade do Algarve, Campus de Gambelas, 8005-139 Faro, Portugal

José P. S. Lemos‡
Centro Multidisciplinar de Astrofísica, CENTRA, Departamento de Física, Instituto Superior Técnico, Av. Rovisco Pais 1, 1049-001 Lisbon, Portugal
(Received 26 January 2004; published 19 July 2004)

We find all higher dimensional solutions of Einstein-Maxwell theory that are the topological product of two manifolds of constant curvature. These solutions include the higher dimensional Nariai, Bertotti-Robinson and anti-Nariai solutions and the anti–de Sitter Bertotti-Robinson solutions with toroidal and hyperbolic topology (Plebański-Hacyan solutions). We give explicit results for any dimension $D \geqslant 4$. These solutions are generated from the appropriate extremal limits of the higher dimensional near-extreme black holes in de Sitter and anti–de Sitter backgrounds. Thus, we also find the mass and charge parameters of higher dimensional extreme black holes as a function of the radius of the degenerate horizon.

DOI: 10.1103/PhysRevD.70.024002 PACS number(s): 04.20.Jb, 04.20.Gz, 04.70.Bw

I. INTRODUCTION

Interest in higher dimensional spacetimes was boosted with the development of string theories. More recently, there has been a renewed interest in connection with the TeV-scale theory [1] which suggests that the universe in which we live may have large extra dimensions. According to this conjecture, we would live on a four-dimensional sub-manifold, where the standard model inhabits, whereas the gravitational degrees of freedom propagate throughout all dimensions. This has motivated a wide search for various phenomena [2] involving higher dimensions. In particular, it is possible that future accelerators, such as the Large Hadron Collider (LHC) at CERN, will produce black holes and thus detect indirectly gravitational waves [3].

In this paper we deal with exact solutions of the Einstein-Maxwell theory in higher dimensions. The higher dimensional counterparts of the Schwarzschild and of the Reissner-Nordström black holes—the Tangherlini black holes—have been found and discussed in [4]. The D-dimensional Majumdar-Papapetrou black holes have been found in [5] (see also [6]). The higher dimensional Kerr black hole—the Myers-Perry black hole—was found in [7] and further discussed in [8]. The higher dimensional counterpart of the Kerr-Newman black hole is not yet known (see [9] for a discussion). The higher dimensional Schwarzschild and Reissner-Nordström black holes in an asymptotically de Sitter (dS) spacetime and in an asymptotically anti–de Sitter (AdS) spacetime have also been discussed in [4]. Now, in an asymptotically AdS 4-dimensional background, besides black holes with spherical topology, there are also solutions with planar, cylindrical or toroidal topology found and discussed in [10] (neutral case), [11] (electric case), and [12] (magnetic case) and black holes [13] with hyperbolic topology analyzed in [14]. The higher dimensional extensions of these non-spherical AdS black holes are already known. Namely, the D-dimensional AdS black holes with planar, cylindrical or toroidal topology were discussed in [15] (neutral case), in [16] (electric case) and in [17] (magnetic case), and the D-dimensional AdS black holes with hyperbolic topology were analyzed in [15,18].

In a 4-dimensional background with generic cosmological constant, and still in the context of Einstein-Maxwell theory, there are other interesting solutions that do not contain a black hole, but are the direct topological product of two manifolds of constant curvature. These are the Nariai solution [20], the Bertotti-Robinson solution [21], the anti-Nariai solution [22], and the Plebański-Hacyan solutions [23]. For a detailed historical overview of these solutions and for references see, e.g., [24–26]. A discussion of these solutions in a more mathematical context can be found in [27]. Some of these solutions, but not all, have already been discussed in a higher dimensional spacetime.

Ginsparg and Perry [28] (see also [29]) have connected the extreme dS-Schwarzschild black hole with the Nariai solution [20] in a 4-dimensional spacetime. That is, they have shown that the already known Nariai solution (which is not a black hole solution) could be generated from an appropriate extremal limit of a near-Nariai black hole. They realized this

*Electronic address: vcardoso@fisica.ist.utl.pt
†Electronic address: oscar@fisica.ist.utl.pt
‡Electronic address: lemos@kelvin.ist.utl.pt

connection while they were studying the quantum stability of the Nariai and the dS-Schwarzschild solutions. A similar procedure allows one to generate the Bertotti-Robinson, the anti-Nariai, and the Plebański-Hacyan solutions from appropriate near-extreme black holes.

In this paper we shall use the procedure introduced in [28] in order to generate, from the appropriate extremal limits of the D-dimensional near-extreme black holes, all the higher dimensional solutions that are the topological product of two manifolds of constant curvature. These solutions include the higher dimensional Nariai, Bertotti-Robinson, anti-Nariai, and Plebański-Hacyan solutions. We give explicit results for any dimension $D \geqslant 4$. In passing we also find the values of the mass and of the charge for which one has extreme black holes in an asymptotically dS and in an asymptotically AdS higher dimensional spacetime. This analysis has already been initiated in [19], but our procedure and results are complementary to those of [19]. In the AdS case, the discussion carried in this paper includes black holes with spherical topology, with planar, cylindrical and toroidal topology, and with hyperbolic topology.

The plan of this paper is as follows. In Sec. II, we set the Einstein-Maxwell action in a D-dimensional background. In Sec. III we discuss the properties of the extreme higher dimensional dS black holes, and we find their extremal limits, i.e. the associated Nariai-like solutions. In Sec. IV we do the same but this time in an AdS background.

II. ACTION AND EQUATIONS OF MOTION

We will discuss solutions that are the extremal limits of the near-extreme cases of the static higher dimensional black holes. Some of these black holes were found by Tangherlini [4] and are the higher dimensional cousins of the Schwarzschild and of the Reissner-Nordström black holes. We work in the context of the Einstein-Maxwell action with a cosmological constant Λ:

$$I=\frac{1}{16\pi}\int_{\mathcal{M}} d^D x\sqrt{-g}\left(R-\frac{(D-1)(D-2)}{3}\Lambda-F^2\right), \quad (1)$$

where D is the dimension of the spacetime, g is the determinant of the metric $g_{\mu\nu}$, R is the Ricci scalar, and $F_{\mu\nu}=\partial_\mu A_\nu-\partial_\nu A_\mu$ is the Maxwell field strength of the gauge field A_ν. We set the D-dimensional Newton's constant equal to 1, and $c=1$. The variation of Eq. (1) yields the equations for the gravitational field and for the Maxwell field, respectively,

$$R_{\mu\nu}-\frac{1}{2}Rg_{\mu\nu}+\frac{(D-1)(D-2)}{6}\Lambda g_{\mu\nu}=8\pi T_{\mu\nu},$$

$$\nabla_\mu F^{\mu\nu}=0, \quad (2)$$

where $R_{\mu\nu}$ is the Ricci tensor and $T_{\mu\nu}$ is the electromagnetic energy-momentum tensor:

$$T_{\mu\nu}=\frac{1}{4\pi}\left(g^{\alpha\beta}F_{\alpha\mu}F_{\beta\nu}-\frac{1}{4}g_{\mu\nu}F_{\alpha\beta}F^{\alpha\beta}\right). \quad (3)$$

In Eq. (1), the coefficient of Λ was chosen in order to ensure that, for any dimension D, the pure dS or pure AdS spacetimes are described by $g_{tt}=1-(\Lambda/3)r^2$, as occurs with $D=4$.

III. HIGHER DIMENSIONAL EXTREME dS BLACK HOLES AND NARIAI-LIKE SOLUTIONS

In order to generate the higher dimensional Nariai, dS-Bertotti-Robinson, and Nariai-Bertotti-Robinson solutions one needs first to carefully find the values of the mass and of the charge for which one has an extreme dS black hole. We will do this in Sec. III A, and in Sec. III B we will generate the Nariai-like solutions from the extremal limits of the near-extreme black holes.

A. Higher dimensional extreme black holes in an asymptotically dS background

In an asymptotically de Sitter background, $\Lambda>0$, the most general static higher dimensional black hole solution with spherical topology was found by Tangherlini [4]. The gravitational field is

$$ds^2=-f(r)dt^2+f(r)^{-1}dr^2+r^2d\Omega_{D-2}^2, \quad (4)$$

where $d\Omega_{D-2}^2$ is the line element on a unit $(D-2)$-sphere,

$$d\Omega_{D-2}^2=d\theta_1^2+\sin^2\theta_1\, d\theta_2^2+\cdots+\prod_{i=1}^{D-3}\sin^2\theta_i d\theta_{D-2}^2, \quad (5)$$

and the function $f(r)$ is given by

$$f(r)=1-\frac{\Lambda}{3}r^2-\frac{M}{r^{D-3}}+\frac{Q^2}{r^{2(D-3)}}. \quad (6)$$

The mass parameter M and the charge parameter Q are related to the Arnowitt-Deser-Misner (ADM) mass, M_{ADM}, and ADM electric charge, Q_{ADM}, of the solution by [7]

$$M_{\mathrm{ADM}}=\frac{(D-2)\Omega_{D-2}}{16\pi}M,$$

$$Q_{\mathrm{ADM}}=\sqrt{\frac{(D-3)(D-2)}{2}}Q, \quad (7)$$

where Ω_{D-2} is the area of a unit $(D-2)$-sphere,

$$\Omega_{D-2}=\frac{2\pi^{(D-1)/2}}{\Gamma[(D-1)/2]}. \quad (8)$$

Here, $\Gamma[z]$ is the gamma function. For our purposes we need to know that $\Gamma[z]=(z-1)!$ when z is a positive integer, $\Gamma[1/2]=\sqrt{\pi}$, and $\Gamma[z+1]=z\Gamma[z]$. The radial electromagnetic field produced by the electric charge Q_{ADM} is given by

$$F=-\frac{Q_{\mathrm{ADM}}}{r^{D-2}}dt\wedge dr. \quad (9)$$

These solutions have a curvature singularity at the origin, and the black hole solutions can have at most three horizons, the Cauchy horizon r_-, the event horizon r_+ and the cosmological horizon r_c, which satisfy $r_- \leqslant r_+ \leqslant r_c$.

We are now interested in the D-dimensional extreme dS-Tangherlini black holes. That is, in order to start searching for Nariai-like solutions one needs first to carefully find the parameters M and Q as a function of the degenerate horizon. To settle the nomenclature and the technical procedure, we start with the five-dimensional case, $D=5$. We look to the extreme dS black holes, for which two of the horizons coincide. Let us label this degenerate horizon by ρ. In this case, and for $D=5$, the function $f(r)$ given by Eq. (6) can be written as

$$f(r)=-\frac{\Lambda}{3}\frac{1}{r^4}(r-\rho)^2(r+\rho)^2\left(r^2-\frac{3}{\Lambda}+2\rho^2\right). \quad (10)$$

Thus, besides the degenerate horizon $r=\rho$, there is another horizon at $\sigma=\sqrt{3/\Lambda-2\rho^2}$. From Eq. (6) with $D=5$ and Eq. (10), the mass parameter M and the charge parameter Q of the black holes can be written as functions of ρ: $M=\rho^2(2-\Lambda\rho^2)$ and $Q^2=\rho^4(1-2\Lambda\rho^2/3)$. The condition $Q^2\geqslant 0$ implies that $\rho\leqslant\sqrt{3/(2\Lambda)}$. At this point we note that M and Q first increase with ρ (this sector corresponds to $\sigma>\rho$), until ρ reaches the critical value $\rho=\sqrt{1/\Lambda}$ (this sector corresponds to $\sigma=\rho$), and then M and Q start decreasing until ρ reaches its maximum allowed value (this sector corresponds to $\sigma<\rho$). These three sectors are associated with three distinct extreme dS black holes: the cold, the ultracold and the Nariai black holes, respectively. (Here we follow the nomenclature used in the analogous 4-dimensional black holes [30]. Note that the Nariai black hole differs from the Nariai solution which is not a black hole solution.) More precisely, for $0<\rho<1/\sqrt{\Lambda}$ one has the cold black hole with $r_-=r_+\equiv\rho$ and $r_c\equiv\sigma$. The ranges of the mass and charge parameters for the cold black hole are $0<M<1/\Lambda$ and $0<Q<1/(\sqrt{3}\Lambda)$. The case $\rho=1/\sqrt{\Lambda}$ gives the ultracold black hole in which the three horizons coincide, $r_-=r_+=r_c$. Its mass and charge parameters are $M=1/\Lambda$ and $Q=1/(\sqrt{3}\Lambda)$. For $1/\sqrt{\Lambda}<\rho\leqslant\sqrt{3/(2\Lambda)}$ one has the Nariai black hole with $r_+=r_c\equiv\rho$ and $r_-\equiv\sigma$. The ranges of the mass and charge parameters for the Nariai black hole are $3/(4\Lambda)\leqslant M<1/\Lambda$ and $0\leqslant Q<1/(\sqrt{3}\Lambda)$.

Now, the above construction can be extended to D-dimensional extreme dS black holes. In the extreme case the function $f(r)$ given by Eq. (6) can be written as

$$f(r)=(r-\rho)^2\frac{1}{r^2}\left[1-\frac{\Lambda}{3}[r^2+h(r)]\right], \quad (11)$$

where $r=\rho$ is the degenerate horizon of the black hole, and

$$h(r)=a+br+\frac{c_1}{r}+\frac{c_2}{r^2}+\cdots+\frac{c_{2(D-4)}}{r^{2(D-4)}}, \quad (12)$$

where $a,b,c_1,\ldots,c_{2(D-4)}$ are constants that can be found through the matching between Eqs. (6) and (12). This procedure yields the mass parameter M and the charge parameter Q of the black holes as a function of ρ:

$$M=2\rho^{D-3}\left(1-\frac{D-2}{D-3}\frac{\Lambda}{3}\rho^2\right),$$

$$Q^2=\rho^{2(D-3)}\left(1-\frac{D-1}{D-3}\frac{\Lambda}{3}\rho^2\right). \quad (13)$$

The condition $Q^2\geqslant 0$ implies that $\rho\leqslant\rho_{\max}$ with

$$\rho_{\max}=\sqrt{\frac{D-3}{D-1}\frac{3}{\Lambda}}. \quad (14)$$

For the D-dimensional cold black hole ($r_-=r_+$), M and Q increase with ρ, and one has

$$0<\rho<\rho_u, \quad 0<M<\frac{4}{D-1}\rho_u^{D-3},$$

$$0<Q<\frac{1}{\sqrt{D-2}}\rho_u^{D-3}, \quad (15)$$

where we have defined

$$\rho_u=\sqrt{\frac{3}{\Lambda}}\frac{D-3}{\sqrt{(D-2)(D-1)}}. \quad (16)$$

For the D-dimensional ultracold black hole ($r_-=r_+=r_c$), one has

$$\rho=\rho_u, \quad M=\frac{4}{D-1}\rho_u^{D-3},$$

$$Q=\frac{1}{\sqrt{D-2}}\ \rho_u^{D-3}. \quad (17)$$

Finally, for the D-dimensional Nariai black hole ($r_+=r_c$), M and Q decrease with ρ, and one has

$$\rho_u<\rho\leqslant\rho_{\max}, \quad \frac{2}{D-1}\rho_{\max}^{D-3}\leqslant M<\frac{4}{D-1}\rho_u^{D-3},$$

$$0\leqslant Q<\frac{1}{\sqrt{D-2}}\rho_u^{D-3}. \quad (18)$$

The ranges of M and Q that represent each one of the above extreme black holes are sketched in Fig. 1. This figure and the associated relations (13)–(18) are not the main results of this paper. However, they constitute results that we had to find in our way into the generation of the Nariai-like solutions. For an alternative and complementary description of the extreme dS-Tangherlini black holes see [19].

The Carter-Penrose diagrams of the D-dimensional dS-Tangherlini black holes are similar to the ones of their 4-dimensional counterparts and are sketched in Fig. 2 in the

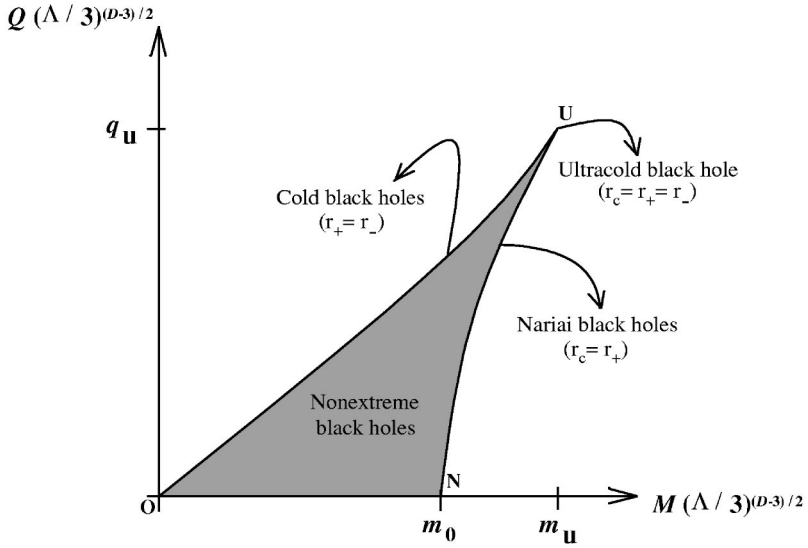

FIG. 1. Range of M and Q for which one has a nonextreme black hole (region interior to the closed line $ONUO$), an extreme Nariai black hole with $r_+=r_c$ (line NU), an extreme cold black hole with $r_-=r_+$ (line OU), and an extreme ultracold black hole with $r_-=r_+=r_c$ (point U). The line ON represents the nonextreme dS-Schwarzschild black hole, and point N represents the extreme Nariai Schwarzschild black hole. The non-shaded area represents a naked singularity region. The constants in the axes are $m_0=[2/(D-1)][(D-3)/(D-1)]^{(D-3)/2}$, $m_u=[4/(D-1)][(D-3)^2/(D-2)\times(D-1)]^{(D-3)/2}$, and $q_u=[1/(\sqrt{D-2})][(D-3)^2/(D-2)(D-1)]^{(D-3)/2}$.

charged case and in Fig. 3 in the neutral case. In these diagrams each point represents a $(D-2)$-sphere of radius r.

B. Extremal limits of the higher dimensional dS black holes

In this section, we apply the near extremal procedure of Ginsparg and Perry [28] to the extreme black holes discussed in the last subsection, in order to find the higher dimensional Nariai, dS-Bertotti-Robinson, $\Lambda=0$ Bertotti-Robinson and Nariai-Bertotti-Robinson solutions. The higher dimensional Nariai solution has already been found in [19,22]. Here we show that it can be generated from the near-Nariai black hole following the procedure of [28]. Therefore, we give emphasis to the solution and we set the nomenclature for the other cases.

1. Higher dimensional Nariai solution

In order to generate the higher dimensional Nariai solution from the near-Nariai black hole we first go back to Eq. (11) and rewrite it in the form $f(r)=-A(r)(r-\rho)^2$, where $r=\rho$ is the degenerate horizon of the black hole, and $A(r)$ is a polynomial function of r. Then, we set $r_+=\rho-\varepsilon$ and $r_c=\rho+\varepsilon$, where $\varepsilon\ll 1$ measures the deviation from degeneracy, and the limit $r_+\to r_c$ is obtained when $\varepsilon\to 0$. Now, we introduce a time coordinate T, $t=T/(\varepsilon A)$ and a radial coordinate χ, $r=\rho+\varepsilon\cos\chi$, where $\chi=0$ and $\chi=\pi$ correspond, respectively, to the horizons r_c and r_+, and $A\equiv A(\rho)=\rho^{-2}[1-(\rho^2+h)\Lambda/3]>0$, with $h\equiv h(\rho)$ defined in Eq. (12). Then, in the limit $\varepsilon\to 0$, from Eqs. (4) and (11), we obtain the gravitational field of the Nariai solution

$$ds^2=\frac{1}{A}(-\sin^2\chi dT^2+d\chi^2)+\frac{1}{B}d\Omega_{D-2}^2, \tag{19}$$

where χ runs from 0 to π, and A and $B=1/\rho^2$ are related to Λ and Q by

$$\Lambda=\frac{3}{(D-2)(D-1)}[A+(D-3)^2B],$$

$$Q^2=\frac{(D-3)B-A}{(D-3)(D-2)B^{D-2}}. \tag{20}$$

The Maxwell field (9) of the higher dimensional Nariai solution is

$$F=Q_{\mathrm{ADM}}\frac{B^{(D-2)/2}}{A}\sin\chi dT\wedge d\chi. \tag{21}$$

So, if we give the parameters Λ and Q, we can construct the higher dimensional Nariai solution, which is an exact solution of Einstein-Maxwell equations (2) with $\Lambda>0$ in D dimensions. Through a redefinition of coordinates, $\sin^2\chi=1-AR^2$ and $\tau=\sqrt{A}T$, the spacetime (19) can be rewritten in static coordinates as

$$ds^2=-(1-AR^2)dT^2+\frac{dR^2}{1-AR^2}+\frac{1}{B}d\Omega_{D-2}^2, \tag{22}$$

and the electromagnetic field changes also accordingly to the coordinate transformation. Written in these coordinates, we clearly see that the Nariai solution is the direct topological product of $dS_2\times S^{D-2}$, i.e. of a $(1+1)$-dimensional dS spacetime with a $(D-2)$-sphere of fixed radius $B^{-1/2}$. This spacetime is homogeneous with the same causal structure as $(1+1)$-dimensional dS spacetime, but it is not an asymptotically 4-dimensional dS spacetime since the radius of the $(D-2)$-sphere is constant $(B^{-1/2})$, contrarily to what happens in the dS solution where this radius increases as one approaches infinity.

The neutral Nariai solution $(Q=0)$ satisfies the relations $A=\Lambda(D-1)/3$ and $B=\Lambda(D-1)/(3D-9)$. The $\Lambda=0$ limit of the Nariai solution is D-dimensional Minkowski spacetime as occurs with the $D=4$ solution (see [26]).

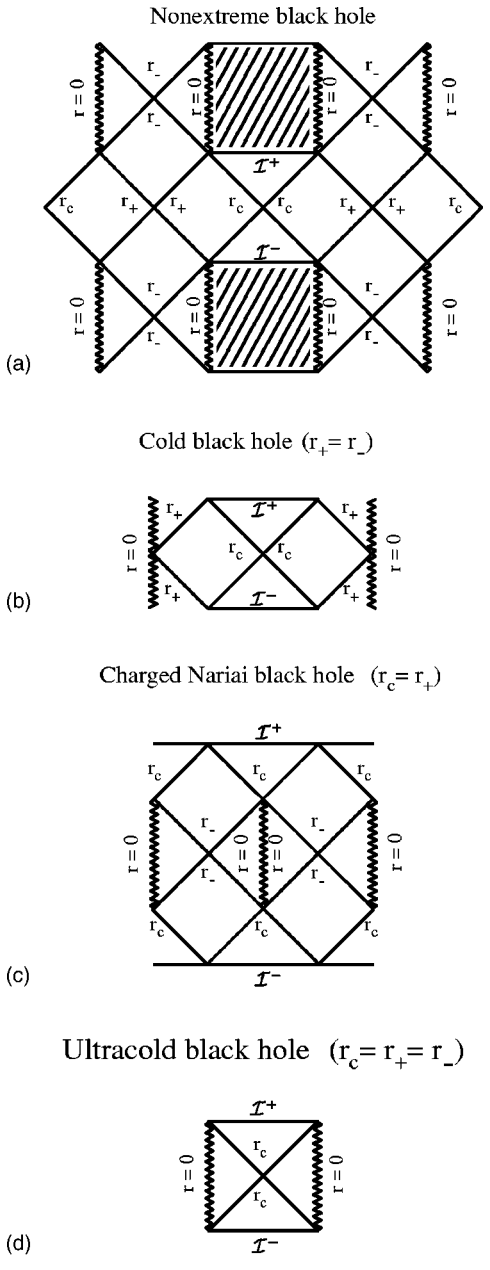

FIG. 2. Carter-Penrose diagrams of the dS-Reissner-Nordström ($Q \neq 0$) black holes. The zigzag line represents a curvature singularity, $\mathcal{I}$ represents the infinity ($r=\infty$), r_c represents a cosmological horizon, r_+ represents a black hole event horizon, and r_- represents a Cauchy horizon. (a) was presented in [31]. As far as we know, (b)–(d) are first shown here.

The Carter-Penrose diagram of the D-dimensional Nariai solution (charged or neutral) is sketched in Fig. 4. In this diagram any point represents a $(D-2)$-sphere with fixed radius $B^{-1/2}$. For a construction that starts with the Carter-Penrose diagram of the dS black hole and leads to the diagram of the Nariai solution see [26].

2. Higher dimensional dS Bertotti-Robinson solution

In order to generate the higher dimensional dS Bertotti-Robinson solution from the near-cold black hole we first go back to Eq. (11) and rewrite it in the form $f(r)=A(r)(r-\rho)^2$, where $r=\rho$ is the degenerate horizon of the black hole, and $A(r)$ is a polynomial function of r. Then, we set $r_-=\rho-\varepsilon$ and $r_+=\rho+\varepsilon$, where $\varepsilon \ll 1$ measures the deviation from degeneracy, and the limit $r_- \to r_+$ is obtained when $\varepsilon \to 0$. Now, we introduce a time coordinate T, $t=T/(\varepsilon A)$, and a new radial coordinate χ, $r=\rho+\varepsilon\cosh\chi$, where $A \equiv A(\rho)=\rho^{-2}[1-\Lambda(\rho^2+h)/3]>0$, with $h \equiv h(\rho)$ defined in Eq. (12). Then, in the limit $\varepsilon \to 0$, from Eqs. (4) and (11), we obtain the gravitational field of the dS Bertotti-Robinson solution

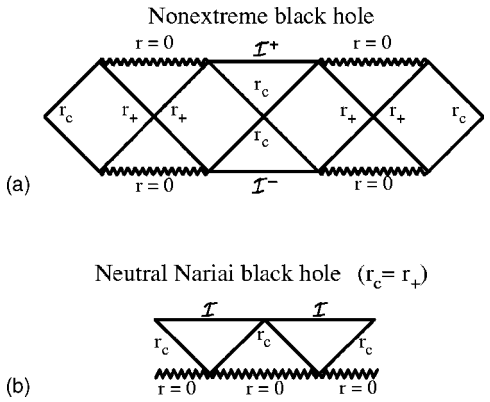

FIG. 3. Carter-Penrose diagrams of the dS-Schwarzschild ($Q=0$) black holes. The zigzag line represents a curvature singularity, $\mathcal{I}$ represents the infinity ($r=\infty$), r_c represents a cosmological horizon, and r_+ represents a black hole event horizon. (a) was presented in [31], and (b) was presented in [32].

$$ds^2=\frac{1}{A}(-\sinh^2\chi dT^2+d\chi^2)+\frac{1}{B}d\Omega^2_{D-2}, \tag{23}$$

where A and $B=1/\rho^2$ are related to Λ and Q by

$$\Lambda=\frac{3}{(D-2)(D-1)}[-A+(D-3)^2B],$$

$$Q^2=\frac{(D-3)B+A}{(D-3)(D-2)B^{D-2}}. \tag{24}$$

The Maxwell field (9) of the higher dimensional dS Bertotti-Robinson solution is

$$F=-Q_{\mathrm{ADM}}\frac{B^{(D-2)/2}}{A}\sinh\chi dT\wedge d\chi. \tag{25}$$

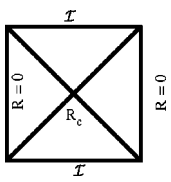

FIG. 4. Carter-Penrose diagram of the Nariai solution (charged or neutral). The zigzag line represents a curvature singularity, $\mathcal{I}$ represents the infinity ($R=\infty$), and R_c represents a cosmological horizon.

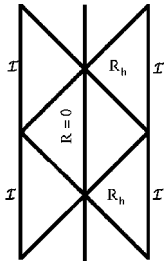

FIG. 5. Carter-Penrose diagram of the Bertotti-Robinson solution in any cosmological constant background. The zigzag line represents a curvature singularity, $\mathcal{I}$ represents the infinity ($R=\infty$), and R_h represents a horizon.

So, if we give the parameters Λ and Q, we can construct the higher dimensional dS Bertotti-Robinson solution, which is an exact solution of Einstein-Maxwell equations (2) with $\Lambda>0$ in D dimensions. There is no neutral ($Q=0$) Bertotti-Robinson solution.

Through a redefinition of coordinates, $\tau=\sqrt{A}T$ and $\sinh^2\chi=AR^2-1$, the spacetime (23) can be rewritten in static coordinates as

$$ds^2=-(AR^2-1)dT^2+\frac{dR^2}{AR^2-1}+\frac{1}{B}d\Omega_{D-2}^2, \quad (26)$$

and the electromagnetic field changes also accordingly to the coordinate transformation. Written in these coordinates, we clearly see that the Bertotti-Robinson solution is the direct topological product of $AdS_2\times S^{D-2}$, i.e. of a $(1+1)$-dimensional AdS spacetime with a $(D-2)$-sphere of fixed radius $B^{-1/2}$.

The Carter-Penrose diagram of the D-dimensional Bertotti-Robinson solution is sketched in Fig. 5. In this diagram any point represents a $(D-2)$-sphere with fixed radius $B^{-1/2}$. For a construction that starts with the Carter-Penrose diagram of the dS black hole and leads to the diagram of the Bertotti-Robinson solution see [26].

The higher dimensional flat Bertotti-Robinson solution is given by the $\Lambda=0$ limit of the dS Bertotti-Robinson. It is described by Eqs. (23) and (25) with A and B being related to Q by

$$A=(D-3)^2Q^{-2/(D-3)}, \quad B=Q^{-2/(D-3)}. \quad (27)$$

Topologically this solution is also $AdS_2\times S^{D-2}$ and is an exact solution of Einstein-Maxwell equations (2) with $\Lambda=0$ in D dimensions. The Carter-Penrose diagram of the higher dimensional flat Bertotti-Robinson solution is also given by Fig. 5.

3. Higher dimensional Nariai-Bertotti-Robinson solution

In order to generate the higher dimensional Nariai-Bertotti-Robinson solution from the near-ultracold black hole we first go back to Eq. (11) and rewrite it in the form $f(r)=-P(r)(r-\rho)^2(r-\sigma)$, where $r=\rho$ is a degenerate horizon of the black hole, $\sigma>\rho$ is the other horizon, and $P(r)$ is a polynomial function of r. Then, we set $\rho=\rho_u-\varepsilon$ and $\sigma=\rho_u+\varepsilon$, with ρ_u defined in Eq. (16) and $\varepsilon\ll 1$ measuring the deviation from degeneracy, and the limit $\rho\to\sigma$ is obtained when $\varepsilon\to 0$. Now, we introduce a new time coordinate T, $t=T/(2\varepsilon^2 P)$, and a radial coordinate χ, $r=\rho_u+\varepsilon\cos(\sqrt{2\varepsilon P}\chi)$, where $P\equiv P(\rho_u)>0$. Then, taking the limit $\varepsilon\to 0$ of Eq. (4), we obtain the gravitational field of the Nariai-Bertotti-Robinson solution, $ds^2=-\chi^2dT^2+d\chi^2+\rho_u^2d\Omega_{D-2}^2$, where χ runs from 0 to $+\infty$, and the Maxwell field (9) of the higher dimensional Nariai-Bertotti-Robinson solution is $F=Q_{ADM}\rho_u^{-D+2}\chi dT\wedge d\chi$. Now, the spacetime factor $-\chi^2dT^2+d\chi^2$ is just $\mathbb{M}^{1,1}$ (2-dimensional Minkowski spacetime) in Rindler coordinates. Therefore, under the usual coordinate transformation $\chi=\sqrt{x^2-t^2}$ and $T=\operatorname{arctanh}(t/x)$, we can write the higher dimensional Nariai-Bertotti-Robinson solution in its simplest form

$$ds^2=-dt^2+dx^2+\rho_u^2d\Omega_{D-2}^2, \quad (28)$$

where ρ_u is defined in Eq. (16), and

$$F=-\frac{Q_{ADM}}{\rho_u^{D-2}}dt\wedge dx, \quad (29)$$

where Q_{ADM} is given by Eqs. (7) and (17). So, if we give Λ we can construct the higher dimensional Nariai-Bertotti-Robinson solution. This solution is the direct topological product of $\mathbb{M}^{1,1}\times S^{D-2}$ and is an exact solution of Einstein-Maxwell equations (2) with $\Lambda>0$ in D dimensions. Its causal diagram is equal to the causal diagram of the Rindler solution. This solution belongs to the class of solutions discussed in detail in [23] (for $D=4$), and thus it can very appropriately be called a Plebański-Hacyan solution [25].

IV. HIGHER DIMENSIONAL EXTREME AdS BLACK HOLES AND ANTI-NARIAI LIKE SOLUTIONS

In order to generate the higher dimensional anti-Nariai, and the two AdS-Bertotti-Robinson solutions one needs first to carefully find the values of the mass and of the charge for which one has extreme AdS black holes. We will do this in Sec. IV A, and in Sec. IV B we will generate the anti-Nariai like solutions from the extremal limits of the near-extreme black holes.

A. Higher dimensional extreme black holes in an asymptotically AdS background

In a higher dimensional asymptotically anti–de Sitter background, $\Lambda<0$, the Einstein-Maxwell equations (2) allow a three-family of static black hole solutions, parametrized by the constant k which can take the values 1, 0, -1, and whose gravitational field is described by

$$ds^2=-f(r)dt^2+f(r)^{-1}dr^2+r^2(d\Omega_{D-2}^k)^2, \quad (30)$$

where

$$f(r)=k-\frac{\Lambda}{3}r^2-\frac{M}{r^{D-3}}+\frac{Q^2}{r^{2(D-3)}}, \quad (31)$$

and for $k=1$, $k=0$ and $k=-1$ one has, respectively,

$$(d\Omega^k_{D-2})^2 = d\theta_1^2 + \sin^2\theta_1 d\theta_2^2 + \cdots + \prod_{i=1}^{D-3} \sin^2\theta_i d\theta_{D-2}^2,$$

$$(d\Omega^k_{D-2})^2 = d\theta_1^2 + d\theta_2^2 + d\theta_3^2 + \cdots + d\theta_{D-2}^2,$$

$$(d\Omega^k_{D-2})^2 = d\theta_1^2 + \sinh^2\theta_1 d\theta_2^2 + \cdots + \prod_{i=1}^{D-3} \sinh^2\theta_i d\theta_{D-2}^2. \tag{32}$$

Thus, the family with $k=1$ yields AdS black holes with spherical topology found in [4]. The family with $k=0$ yields AdS black holes with planar, cylindrical or toroidal (with genus $g \geqslant 1$) topology that are the higher dimensional counterparts (introduced in [15,16]) of the 4-dimensional black holes found and analyzed in [10,11]. Finally, the family with $k=-1$ yields AdS black holes with hyperbolic or toroidal topology with genus $g \geqslant 2$ that are the higher dimensional counterparts (introduced in [15,18] in the neutral case) of the 4-dimensional black holes analyzed in [14]. The solutions with non-spherical topology (i.e. with $k=0$ and $k=-1$) do not have counterparts in a $\Lambda=0$ or in a $\Lambda>0$ background.

The mass parameter M and the charge parameter Q are related to the ADM hairs, $M_{\rm ADM}$ and $Q_{\rm ADM}$, by Eqs. (7). These black holes can have at most two horizons. Following a similar procedure as the one sketched in Sec. III A, we find the mass parameter M and the charge parameter Q of the extreme black holes as a function of the degenerate horizon at $r=\rho$:

$$M = 2\rho^{D-3}\left(k - \frac{D-2}{D-3}\frac{\Lambda}{3}\rho^2\right),$$

$$Q^2 = \rho^{2(D-3)}\left(k - \frac{D-1}{D-3}\frac{\Lambda}{3}\rho^2\right). \tag{33}$$

This equation is not the main result of Sec. IV. However, it constitutes a result that we had to find in our way to the generation of the anti-Nariai like solutions. For an alternative and complementary description of the extreme AdS black holes in D dimensions see [19]. For $D=5$, and only in this case, we were able to write $f(r)$ in the extreme case as a function of the degenerate horizon ρ. We write this expression here since it might be useful for future work:

$$f(r) = -\frac{\Lambda}{3}\frac{1}{r^4}(r-\rho)^2(r+\rho)^2\left(r^2 + 2\rho^2 - k\frac{3}{\Lambda}\right). \tag{34}$$

For $D \geqslant 6$ we were not able to write $f(r)$ as a function of ρ since one has to deal with polynomial functions with degree higher than 4.

1. Higher dimensional AdS black holes with spherical topology

When $k=1$, one has $0<\rho<+\infty$ and M and Q in Eq. (33) are positive parameters. The ranges of M and Q that represent extreme and nonextreme black holes are sketched in Fig. 6.

The Carter-Penrose diagram of the nonextreme AdS-Reissner-Nordström black hole is sketched in Fig. 7(a), and the one of the extreme AdS-Reissner-Nordström black hole is represented in Fig. 7(b). The Carter-Penrose diagram of the AdS-Schwarzschild black hole is drawn in Fig. 8. In these diagrams each point represents a $(D-2)$-sphere of radius r.

2. Higher dimensional AdS black holes with toroidal, cylindrical or planar topology

When $k=0$, one has $0<\rho<+\infty$, and M and Q in Eqs. (33) are positive parameters. The ranges of M and Q that represent extreme and nonextreme black holes are sketched in Fig. 6.

The Carter-Penrose diagram of the nonextreme charged AdS black hole with $k=0$ is sketched in Fig. 7(a), and the one of the extreme charged AdS black hole with $k=0$ is represented in Fig. 7(b). The Carter-Penrose diagram of the neutral AdS black hole with $k=0$ is drawn in Fig. 8. In these diagrams each point represents a $(D-2)$-plane or a $(D-2)$-cylinder or a $(D-2)$-torus.

3. Higher dimensional AdS black holes with hyperbolic topology

When $k=-1$, the condition that $Q^2 \geqslant 0$ demands that $\rho_{\rm min} \leqslant \rho < +\infty$, where

$$\rho_{\rm min} = \sqrt{-\frac{D-3}{D-1}\frac{3}{\Lambda}}. \tag{35}$$

For $\rho=\rho_{\rm min}$, the extreme black hole has no electric charge $(Q=0)$ and its mass is negative, $M=-4\rho_{\rm min}^{D-3}/(D-1)$. For $\rho=\rho_0$, where

$$\rho_0 = \sqrt{-\frac{D-3}{D-2}\frac{3}{\Lambda}}, \tag{36}$$

the extreme black hole has no mass $(M=0)$ and its charge is given by $Q=\rho_0^{D-3}/\sqrt{D-2}$. The ranges of M and Q that represent extreme and nonextreme black holes are sketched in Fig. 9.

In what concerns the causal structure of these solutions, when $M=0$ and $Q=0$, the solution has a horizon that we identify as a cosmological horizon (r_c) since it is present when the mass and charge vanish. In this case $r=0$ is not a curvature singularity, but can be regarded as a topological singularity (see Brill, Louko, and Peldan in [14] for a detailed discussion). The Carter-Penrose diagram of this solution is drawn in Fig. 10, as long as we interpret the zigzag line as being a topological singularity. When $Q=0$ and $M>0$, the solution still has a single horizon, the same cosmological horizon that is present in the latter case. However, now a curvature singularity is present at $r=0$. The corresponding Carter-Penrose diagram of this solution is represented in Fig. 10. The most interesting $Q=0$ solutions are present when their mass is negative. In this case one can have a black hole solution with a black hole horizon and a cosmological horizon [see Fig. 11(a)] or an extreme black hole, in which the two above horizons merge [see Fig.

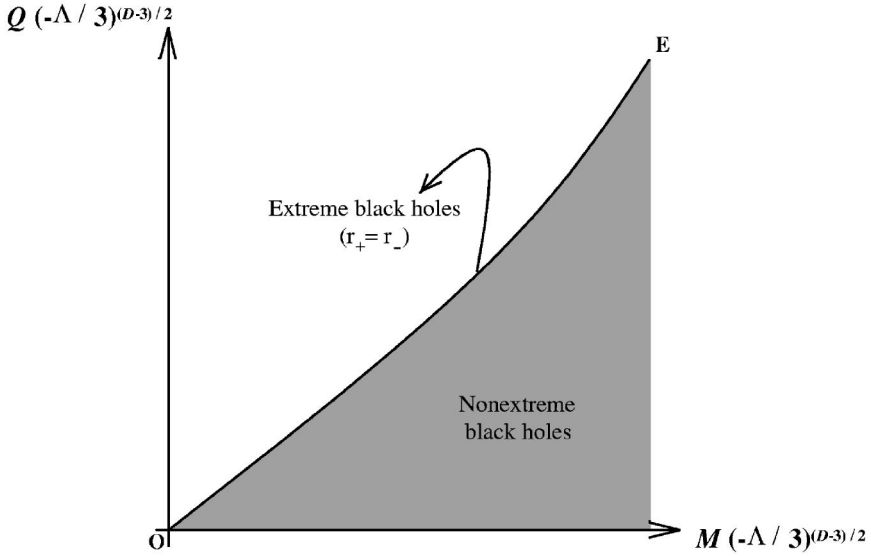

FIG. 6. Range of M and Q for which one has a nonextreme black hole (shaded region) and an extreme black hole with $r_+=r_-$ (line OE) in the AdS case with spherical topology ($k=1$) or with planar, cylindrical or toroidal topology ($k=0$). The non-shaded region represents naked singularities.

11(b)]. When $Q\neq 0$, one can have a black hole solution with a black hole horizon and a cosmological horizon [see Fig. 11(a) for the corresponding causal diagram] or an extreme black hole, in which the two above horizons merge [see Fig. 11(b) for the corresponding causal diagram]. Note that the presence of the charge does not introduce an extra horizon, contrary to what usually occurs in the other black hole solutions.

B. Extremal limits of the higher dimensional AdS black holes

In this subsection, we will consider the extremal limits of the near-extreme higher dimensional AdS black holes. This procedure leads to the generation of the higher dimensional anti-Nariai solution and to the higher dimensional AdS Bertotti-Robinson solutions. To achieve our aim, we first go back to the extreme case of (31) and rewrite it in the form $f(r)=A(r)(r-\rho)^2$, where $r=\rho$ is the degenerate horizon of the black hole, and $A(r)$ is a polynomial function of r. Then, we introduce a new time coordinate T, $t=T/(\varepsilon A)$, and a new radial coordinate χ, $r=\rho+\varepsilon\cosh\chi$, where $A\equiv A(\rho)$, and $\varepsilon \ll 1$ measures the deviation from degeneracy. Finally, taking the limit $\varepsilon\to 0$ in Eq. (30) yields the gravitational field of the higher dimensional solutions:

$$ds^2=\frac{1}{A}(-\sinh^2\chi dT^2+d\chi^2)+\frac{1}{B}(d\Omega^k_{D-2})^2, \qquad (37)$$

where $k=1,0,-1$ in the spherical, cylindrical and hyperbolic cases, respectively, and A and B are constants related to Λ and Q by

$$\Lambda=-\frac{3}{(D-2)(D-1)}[A-k(D-3)^2B],$$

$$Q^2=\frac{A+k(D-3)B}{(D-3)(D-2)B^{D-2}}. \qquad (38)$$

In the coordinate system, the Maxwell field (9) of the solutions is

$$F=-Q_{\rm ADM}\frac{B^{(D-2)/2}}{A}\sinh\chi dT\wedge d\chi. \qquad (39)$$

Equations (37)–(39) describe three exact solutions of the

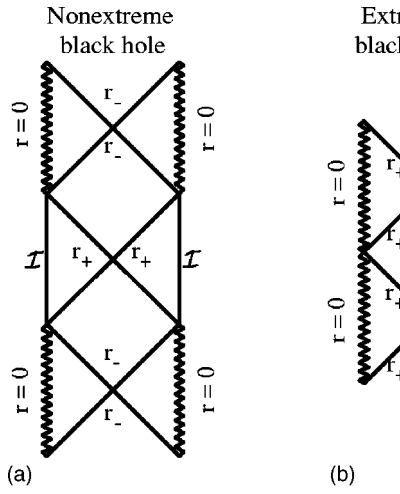

FIG. 7. Carter-Penrose diagrams of the charged ($Q\neq 0$) AdS black holes with $k=1$ and $k=0$. The zigzag line represents a curvature singularity, $\mathcal{I}$ represents the infinity ($r=\infty$), r_+ represents a black hole event horizon, and r_- represents a Cauchy horizon.

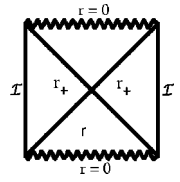

FIG. 8. Carter-Penrose diagrams of the neutral ($Q=0$) AdS black holes with $k=1$ and $k=0$. The zigzag line represents a curvature singularity, $\mathcal{I}$ represents the infinity ($r=\infty$), and r_+ represents a black hole event horizon.

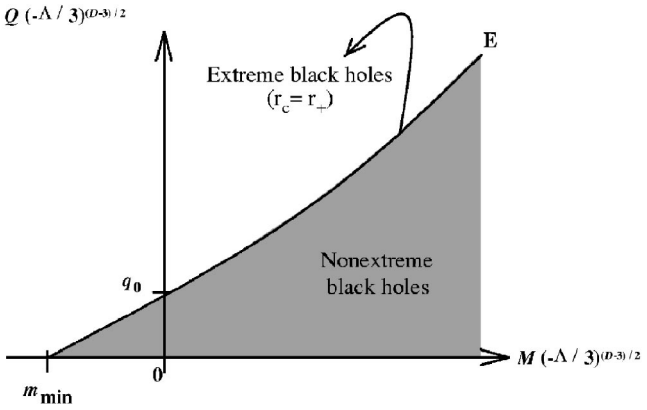

FIG. 9. Range of M and Q for which one has a nonextreme black hole and an extreme black hole with $r_c=r_+$ in the AdS case with hyperbolic topology ($k=-1$). The non-shaded region represents a naked singularity. One has $m_{\min}=-[4/(D-1)][(D-3)/(D-2)]^{(D-3)/2}$ and $q_0=[(D-3)/(D-2)]^{(D-3)/2}/\sqrt{D-2}$.

Einstein-Maxwell equations (2) with $\Lambda<0$ in D dimensions, which we discuss in the following subsections.

1. Higher dimensional AdS Bertotti-Robinson solution with spherical topology

The $k=+1$ case describes the AdS Bertotti-Robinson solution with spherical topology. This solution is the direct topological product of $\mathrm{AdS}_2\times S^{D-2}$, i.e. of a $(1+1)$-dimensional AdS spacetime with a $(D-2)$-sphere of fixed radius $B^{-1/2}$. The Carter-Penrose diagram of this D-dimensional spherical AdS Bertotti-Robinson solution is sketched in Fig. 5. In this diagram any point represents a $(D-2)$-sphere with fixed radius $B^{-1/2}$.

2. Higher dimensional AdS Bertotti-Robinson solution with toroidal, cylindrical or planar topology

The $k=0$ case describes the AdS Bertotti-Robinson solution with toroidal, cylindrical or planar topology, also known as Plebański-Hacyan solution [23]. This solution is the direct topological product of $\mathrm{AdS}_2\times\mathbb{E}^{D-2}$, i.e. of a $(1+1)$-dimensional AdS spacetime with a $(D-2)$ Euclidean space. The Carter-Penrose diagram of this D-dimensional toroidal Bertotti-Robinson solution is sketched in Fig. 5.

In this diagram any point represents a $(D-2)$-plane, a $(D-2)$-cylinder, or a $(D-2)$-torus with fixed size.

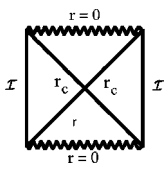

FIG. 10. Carter-Penrose diagrams of the neutral AdS black holes with $k=-1$. The zigzag line represents a curvature singularity, $\mathcal{I}$ represents the infinity ($r=\infty$), r_+ represents a black hole event horizon, and r_- represents a Cauchy horizon.

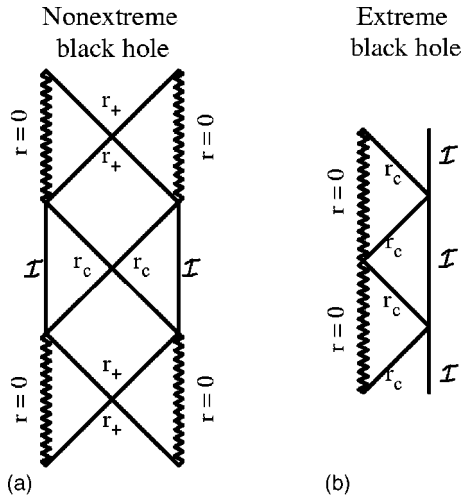

FIG. 11. Carter-Penrose diagrams of the charged AdS black holes with $k=-1$. The zigzag line represents a curvature singularity, $\mathcal{I}$ represents the infinity ($r=\infty$), r_+ represents a black hole event horizon, and r_- represents a Cauchy horizon.

3. Higher dimensional anti-Nariai solution

Finally, the $k=-1$ case describes the higher dimensional anti-Nariai solution. This solution is the direct topological product of $\mathrm{AdS}_2\times H^{D-2}$, i.e. of a $(1+1)$-dimensional AdS spacetime with a $(D-2)$-hyperboloid with a fixed size, $B^{-1/2}$. The $k=-1$ case is the only one that admits a solution with $Q=0$. This neutral anti-Nariai solution satisfies $A=-\Lambda(D-1)/3$ and $B=-\Lambda(D-1)/(3D-9)$. The $\Lambda=0$ limit of the anti-Nariai solution is D-dimensional Minkowski spacetime as occurs with the $D=4$ solution (see [26]). The Carter-Penrose diagram of this D-dimensional anti-Nariai solution is sketched in Fig. 5. In this diagram any point represents a $(D-2)$-hyperboloid with fixed size, $B^{-1/2}$.

V. CONCLUSION

We have constructed all the higher dimensional solutions that are the topological product of two manifolds of constant curvature and that can be generated from the extremal limits of the near-extreme black holes. Our analysis yields explicit results that apply to any dimension $D\geqslant 4$. These solutions include the D-dimensional counterparts of the well-known Nariai, Bertotti-Robinson, anti-Nariai, and Plebański-Hacyan solutions. In order to achieve our aim we had to find the values of the mass and of the charge for which one has extreme black holes in an asymptotically de Sitter and in an asymptotically anti–de Sitter higher dimensional spacetime. This is not an easy task in a D-dimensional background since one has to deal with polynomial functions with degree higher than four.

Nowadays, one of the main motivations to study higher dimensional asymptotically AdS or dS black holes is related with the AdS/CFT and dS/CFT correspondences. In particular, the higher dimensional cosmological black holes are useful to study the dynamics of Friedmann-Robertson-Walker branes in the framework of (A)dS/CFT correspondence (for a review see, e.g., [33]). The solutions discussed in this paper,

being extremal limits of higher dimensional black holes, might also be interesting in this context. They might also be useful for the discussion of modified gravities. Another research area that might follow from this paper is the study of impulsive waves in the background of the spacetimes that we presented, in a direct generalization of the analysis done for four dimensions in [25]. As a last example of application of these higher dimensional solutions, we mention the study of their classical stability, i.e. the exact analytical analysis of their quasinormal modes. Finally, the quantum stability of these Nariai-like solutions will be discussed in [34].

ACKNOWLEDGMENTS

The authors would like to thank Marcello Ortaggio for a critical reading of the manuscript and for pointing out their attention to Refs. [23,27]. This work was partially funded by Fundação para a Ciência e Tecnologia (FCT) through project CERN/FIS/43797/2001 and PESO/PRO/2000/4014. V.C. and O.J.C.D. also acknowledge financial support from the FCT through the PRAXIS XXI program. J.P.S.L. thanks Observatório Nacional do Rio de Janeiro for hospitality.

[1] N. Arkani-Hamed, S. Dimopoulos, and G. Dvali, Phys. Lett. B **429**, 263 (1998); Phys. Rev. D **59**, 086004 (1999); I. Antoniadis, N. Arkani-Hamed, S. Dimopoulos, and G. Dvali, Phys. Lett. B **436**, 257 (1998).

[2] A.O. Barvinsky and S.N. Solodukhin, Nucl. Phys. **B675**, 159 (2003); V. Cardoso, S. Yoshida, O.J.C. Dias, and J.P.S. Lemos, Phys. Rev. D **68**, 061503(R) (2003); V. Cardoso, O.J.C. Dias, and J.P.S. Lemos, *ibid.* **67**, 064026 (2003).

[3] P.C. Argyres, S. Dimopoulos, and J. March-Russell, Phys. Lett. B **441**, 96 (1998); S. Dimopoulos and G. Landsberg, Phys. Rev. Lett. **87**, 161602 (2001). Neutrino cosmic rays could also provide observable examples of black hole production in high-energy particle collisions. See, for example, J.L. Feng and A.D. Shapere, *ibid.* **88**, 021303 (2002).

[4] F.R. Tangherlini, Nuovo Cimento **27**, 636 (1963).

[5] R.C. Myers, Phys. Rev. D **35**, 455 (1987).

[6] J.P.S. Lemos and V.T. Zanchin (in preparation).

[7] R.C. Myers and M.J. Perry, Ann. Phys. (N.Y.) **172**, 304 (1986).

[8] R. Emparan and R.C. Myers, J. High Energy Phys. **09**, 025 (2003).

[9] D. Ida and Y. Uchida, Phys. Rev. D **68**, 104014 (2003).

[10] J.P.S. Lemos, Class. Quantum Grav. **12**, 1081 (1995); Phys. Lett. B **353**, 46 (1995); P.M. Sá, A. Kleber, and J.P.S. Lemos, Class. Quantum Grav. **13**, 125 (1996); P.M. Sá and J.P.S. Lemos, Phys. Lett. B **423**, 49 (1998).

[11] J.P.S. Lemos and V.T. Zanchin, Phys. Rev. D **54**, 3840 (1996); O.J.C. Dias and J.P.S. Lemos, *ibid.* **64**, 064001 (2001).

[12] O.J.C. Dias and J.P.S. Lemos, Class. Quantum Grav. **19**, 2265 (2002); Phys. Rev. D **66**, 024034 (2002).

[13] D. Klemm, V. Moretti, and L. Vanzo, Phys. Rev. D **57**, 6127 (1998).

[14] S. Åminnenborg, I. Bengtsson, S. Holst, and P. Peldán, Class. Quantum Grav. **13**, 2707 (1996); D.R. Brill, Helv. Phys. Acta **69**, 249 (1996); S.L. Vanzo, Phys. Rev. D **56**, 6475 (1997); D.R. Brill, J. Louko, and P. Peldán, *ibid.* **56**, 3600 (1997); R.B. Mann, Class. Quantum Grav. **14**, 2927 (1997); S. Holst and P. Peldan, *ibid.* **14**, 3433 (1997).

[15] D. Birmingham, Class. Quantum Grav. **16**, 1197 (1999); R.G. Cai and K.S. Soh, Phys. Rev. D **59**, 044013 (1999).

[16] A. Chamblin, R. Emparan, C.V. Johnson, and R.C. Myers, Phys. Rev. D **60**, 064018 (1999); **60**, 104026 (1999); A.M. Awad, Class. Quantum Grav. **20**, 2827 (2003).

[17] M.H. Dehghani, Phys. Rev. D **69**, 044024 (2004).

[18] M.H. Dehghani, Phys. Rev. D **65**, 124002 (2002); **65**, 104003 (2002).

[19] H. Kodama and A. Ishibashi, Prog. Theor. Phys. **111**, 29 (2004).

[20] H. Nariai, Sci. Rep. Tohoku Univ., Ser. 1 **34**, 160 (1950); **35**, 62 (1951).

[21] B. Bertotti, Phys. Rev. **116**, 1331 (1959); I. Robinson, Bull. Acad. Pol. Sci., Ser. Sci., Math., Astron. Phys. **7**, 351 (1959).

[22] M. Caldarelli, L. Vanzo, and Z. Zerbini, in *Geometrical Aspects of Quantum Fields*, edited by A.A. Bytsenko, A.E. Gonçalves, and B.M. Pimentel (World Scientific, Singapore, 2001); N. Dadhich, gr-qc/0003026.

[23] J.F. Plebański and S. Hacyan, J. Math. Phys. **20**, 1004 (1979).

[24] S. Nojiri and S.D. Odintsov, Int. J. Mod. Phys. A **14**, 1293 (1999); Phys. Rev. D **59**, 044026 (1999); R. Bousso, *ibid.* **58**, 083511 (1998); hep-th/0205177.

[25] M. Ortaggio, Phys. Rev. D **65**, 084046 (2002); M. Ortaggio and J. Podolský, Class. Quantum Grav. **19**, 5221 (2002); **20**, 1685 (2003).

[26] O.J.C. Dias and J.P.S. Lemos, Phys. Rev. D **68**, 061503(R) (2003).

[27] F.A. Ficken, Ann. Math. **40**, 892 (1939); M. Cahen and L. Defrise, Commun. Math. Phys. **11**, 56 (1968).

[28] P. Ginsparg and M.J. Perry, Nucl. Phys. **B222**, 245 (1983).

[29] S.W. Hawking and S.F. Ross, Phys. Rev. D **52**, 5865 (1995); R.B. Mann and S.F. Ross, *ibid.* **52**, 2254 (1995).

[30] L.J. Romans, Nucl. Phys. **B383**, 395 (1992).

[31] G. Gibbons and S. Hawking, Phys. Rev. D **15**, 2738 (1977).

[32] K. Lake and R. Roeder, Phys. Rev. D **15**, 3513 (1977).

[33] S. Nojiri and S.D. Odintsov, J. High Energy Phys. **12**, 033 (2001); S. Nojiri, S.D. Odintsov, and S. Ogushi, Phys. Rev. D **65**, 023521 (2002); Int. J. Mod. Phys. A **17**, 4809 (2002).

[34] V. Cardoso, O.J.C. Dias, and J.P.S. Lemos (unpublished).